Reaction Chemistry & Engineering

ROYAL SOCIETY OF CHEMISTRY

PAPER

View Article Online
View Journal

Cite this: DOI: 10.1039/d6re00130k

Integrated continuous-flow process for acetaminophen synthesis: hydrogenation of 4-nitrophenol, gas–liquid–liquid separation, acetylation, and crystallisation

Kwihwan Kobayashi, * Shingo Komatsuzaki, Takenori Kimura and Akira Yada

Received 13th April 2026,
Accepted 12th June 2026

DOI: 10.1039/d6re00130k

rsc.li/reaction-engineering

We developed a continuous process for synthesising acetaminophen, an analgesic and antipyretic pharmaceutical, *via* flow hydrogenation of 4-nitrophenol, inline separation, flow acetylation, and crystallisation. Although continuous synthesis has been explored, existing processes face challenges related to catalyst handling, solvent use, and crystallisation integration. Scalable flow hydrogenation was achieved by simultaneously reducing 4-nitrophenol dissolved in an organic solvent and neutralizing it with aqueous acetic acid in a packed column containing bead-type Pd/AmberlystA21; Amberlyst A21 is a neutral ion-exchange resin. Following inline gas–liquid–liquid separation, acetylation was performed in a plug flow reactor, and subsequent crystallisation enabled the isolation of acetaminophen in crystalline form. The process achieved a productivity of 155.0 g h^{-1} and process mass intensity of 23.8, demonstrating its efficiency and scalability. This study aimed to develop a fully continuous, scalable route that integrates hydrogenation, acetylation, and crystallisation without requiring concentration steps. These findings demonstrate the feasibility of a safer, greener, and more scalable pathway for acetaminophen manufacturing.

Introduction

Acetaminophen (AcAP) is a widely used analgesic and antipyretic pharmaceutical included in the WHO essential medicines list.[1] Considering the recent COVID-19 pandemic, during which AcAP was widely prescribed as an antipyretic for symptom management, the development of an efficient production process for AcAP has become increasingly important. A promising green and sustainable synthetic route involves the reduction of 4-nitrophenol (4-NP)—derived from phenol, a depolymerisation product of lignin—into 4-aminophenol (4-AP),[2–4] followed by acetylation to yield AcAP, thereby valorising lignin as a renewable resource and reducing reliance on fossil-derived feedstocks.[5–9] Accordingly, a scalable process for acetaminophen production is desired. Conventionally, 4-NP reduction is achieved *via* a Béchamp-type reaction using metals and acids, generating stoichiometric amounts or excess metal waste.[10–13] Recently, hydrogen gas (H_2) has gained attention as a green reducing agent,[14–16] and its use in catalytic hydrogenation with heterogeneous metal catalysts represents a more sustainable approach.[17–24] However, because of the explosive nature of hydrogen gas, scaling up the reaction requires specialised, high-safety facilities, which leads to higher equipment costs. To address this issue, packed-bed flow reactors filled with heterogeneous catalysts have attracted attention.[25–29] Because hydrogenation occurs within a column, the safety concerns associated with batch processes can be mitigated in flow systems. Therefore, if both hydrogenation and acetylation of 4-NP can be performed in a flow system, AcAP can be produced in a green and sustainable manner. Recently, Sievers and Bommarius reported a flow process for AcAP synthesis using 4-NP as the starting material (Fig. 1a).[30] Their method employed acetic anhydride (Ac_2O) as the acetylating agent and performed both hydrogenation and acetylation in the reaction columns, achieving a highly efficient process with a remarkably low process mass intensity (PMI) of 7.2. However, the use of powdered palladium on alumina (Pd/Al_2O_3) catalysts raises concerns about excessive pressure drops during column scale-up. In addition, methanol was used as the reaction solvent, necessitating a concentration step prior to crystallisation. Concentration steps are often avoided in process development because of their high energy consumption, the need for expensive equipment, and the potential to reduce the throughput, especially in continuous flow systems.[31–33] Therefore, we aimed to develop a continuous

Catalytic Chemistry Research Institute, National Institute of Advanced Industrial Science and Technology (AIST), Higashi 1-1-1, Tsukuba, Ibaraki 305-8565, Japan. E-mail: kobayashi-kwihwan@aist.go.jp

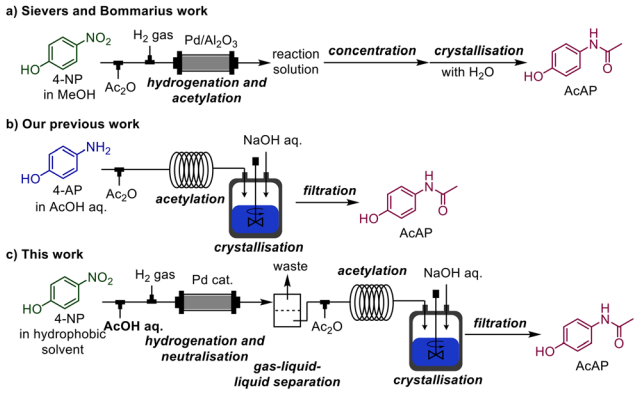

Fig. 1 Comparison of different process strategies for the synthesis of AcAP. (a) The work of Sievers and Bommarius involving hydrogenation and acetylation using Pd/Al_2O_3, followed by concentration and crystallisation. (b) Our previous work using acetylation in aqueous media followed by crystallisation. (c) The process developed in this study, integrating hydrogenation, neutralisation, acetylation, gas–liquid–liquid separation, and crystallisation.

production process for AcAP from 4-NP that fully incorporates the crystallisation step.

We recently developed a process for AcAP synthesis using 4-AP as the starting material and water as a green solvent (Fig. 1b).[34] By converting poorly soluble 4-AP into its acetate salt, it could be utilised as an aqueous solution. After acetylation, subsequent neutralisation with aqueous sodium hydroxide (NaOH) enabled the efficient recovery of AcAP. Thus, if 4-NP could be converted into an aqueous acetate solution of 4-AP, a continuous production process—including crystallisation[35–38]—could be established. However, since 4-NP is almost insoluble in water, establishing a process using 4-NP as the starting material in a green water solvent is not feasible. Therefore, we focused on the basicity difference between 4-NP and 4-AP (Fig. 1c). A hydrophobic organic solution of 4-NP, aqueous acetic acid, and H_2 was simultaneously introduced into a packed column containing the Pd catalyst. Within the column, nitro-group reduction and acetate formation proceeded concurrently, transferring the resulting 4-AP acetate into the aqueous phase. Subsequent gas–liquid–liquid separation yielded an aqueous acetate solution of 4-AP, which was then subjected to acetylation and crystallisation *via* acetic-acid neutralisation, completing the continuous production process for AcAP.

Results and discussion

Flow hydrogenation of 4-NP using packed-bed reactor

First, the continuous flow hydrogenation of 4-NP (**1**) to 4-AP (**2**) was investigated (Table 1). A solution of **1** in ethyl acetate (AcOEt) or butyl acetate (AcOBu) (2 M) and aq. acetic acid (AcOH) (1.8 M) was prepared. A reaction column (ID: 10 mm; *L*: 100 mm) was packed with 5%Pd/Al_2O_3 (Tokyo Chemical Industry Co. Ltd.) and Wakogel C-400 silica gel (particle size: 20–40 μm; FUJIFILM Wako Pure Chemical Corporation) in a 1 : 20 ratio. The solubility of **1** in other hydrophobic organic solvents, such as toluene and heptane, is lower than that in AcOEt and AcOBu. Solutions of **1** and AcOH were pumped at 0.3 and 0.6 mL min^{-1}, respectively, and merged using a connector. H_2 gas was supplied at 60 mL min^{-1} and merged with the reaction solution. The mixed liquid and gas streams were passed through a pressure gauge, and the reaction

Table 1 Optimisation of continuous-flow hydrogenation of **1**

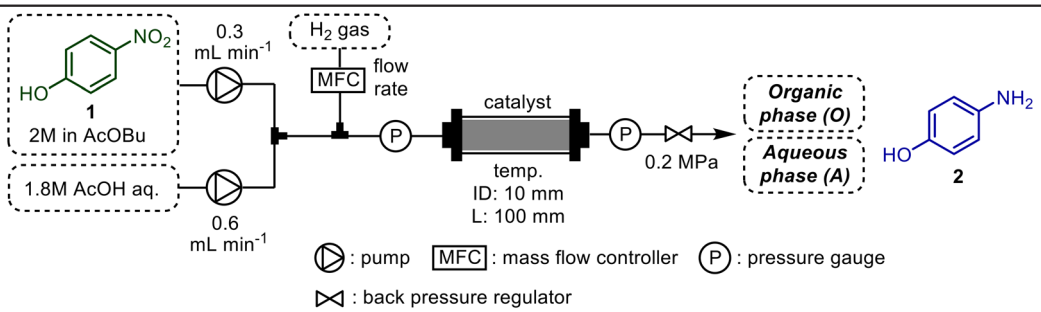

Entry	Temperature (°C)	Flow rate (mL min^{-1})	Catalyst	Δ*P* (MPa)	Conversion (%)	Yield in *O* (%)	Yield in *A* (%)
1[a]	40	60	5%Pd/Al_2O_3 : wakogelC-400 (1 : 20)	0.22	90	9	81
2	40	60	5%Pd/Al_2O_3 : wakogelC-400 (1 : 20)	0.22	88	2	86
3	40	60	5%Pd/Al_2O_3 : wakogelC-200 (1 : 20)	0.10	85	3	82
4	40	60	5%Pd/Al_2O_3 : wakogelC-200 (1 : 10)	0.10	94	3	91
5	40	65	5%Pd/Al_2O_3 : wakogelC-200 (1 : 10)	0.10	96	3	93
6	40	70	5%Pd/Al_2O_3 : wakogelC-200 (1 : 10)	0.10	98	3	95
7[b]	40	210	5%Pd/Al_2O_3 : wakogelC-200 (1 : 10)	0.40	99	2	77
8	80	70	0.6%Pd/CARiACT Q-3	0.01	54	2	52
9	80	70	0.6%Pd/Al_2O_3 beads	0.01	52	1	51
10	80	70	0.6%Pd/MS3A (spherical)	0.01	90	4	86
11	80	70	0.6%Pd/Amberlyst A21	0.02	99	4	96

[a] AcOEt was used instead of AcOBu. [b] Flow rates of **1** and AcOH solutions were 0.9 and 1.8 mL min^{-1}, respectively. The reaction column dimensions were: ID = 10 mm and *L* = 300 mm.

column was heated at 40 °C. The reaction mixture was passed through another pressure gauge and a back-pressure regulator. The resulting organic phase (*O*) and aqueous phase (*A*) were separately analysed by high-performance liquid chromatography (HPLC, analysis conditions were provided in SI) to determine conversion and the yield of **2** in each phase. Two pressure gauges were installed upstream and downstream of the reaction column to monitor the differential pressure (Δ*P*).

When AcOEt was used as the organic solvent (entry 1, Table 1), the conversion of **1** was 90% and the yields of **2** in *O* and *A* were 9% and 81%, respectively. To increase the yield of **2** in *A*, the more hydrophobic AcOBu was used, resulting in 2% and 86% yield of **2** in *O* and *A* respectively (entry 2, Table 1). In entries 1 and 2, Δ*P* was 0.22 MPa; therefore, scaling up this reaction system could result in an excessive Δ*P*. To address this, the dilutant for the Pd catalyst in the reaction column was changed to Wakogel C-200 (particle size: 75–150 μm), reducing Δ*P* to 0.10 MPa (entry 3, Table 1). To further improve the conversion and yield, the amounts of the Pd catalyst and H_2 gas were increased, resulting in improved conversion and an increased yield of **2** in *A* to 98% and 95%, respectively (entries 4–6, Table 1). In entry 7, scale-up experiments were attempted using a reaction column with 3-fold length (ID: 10 mm, *L*: 300 mm) and 3-fold increased flow rates of the solution and gas. However, Δ*P* increased sharply to 0.40 MPa, and the yield of **2** in *A* decreased to 77% due to hydrogenation of the aromatic rings derived from **2**. Under these reaction conditions, employing powdered catalysts in the reaction column was anticipated to increase the Δ*P*, making further scale-up experiments difficult. Therefore, we decided to employ bead-form catalyst to avoid excessive Δ*P*. The preparation procedure for the bead-form Pd catalysts is provided in the SI. The following catalyst supports were selected: CARiACT Q-3 (Fiji Silysia Chemical Ltd., particle size 1.18–2.26 mm), Al_2O_3 beads (Sumitomo Chemical Company Ltd., KHO-12, particle size 1.0–2.0 mm), MS3A (FUJIFILM Wako Pure Chemical Corporation, particle size 1.4–2.0 mm), and AmberlystA21 (Merck & Co., particle size 0.49–0.69 mm). Beads prepared from the Pd catalysts were packed into the reaction column without dilutants, and their reactivity was examined. The 0.6%Pd/CARiACT Q-3 and Al_2O_3 beads resulted in moderate yield of **2** in *A* with a Δ*P* of 0.01 MPa (entries 8 and 9, Table 1). The 0.6%Pd/MS3A catalyst also afforded a good yield of **2** (entry 10, Table 1). In the case of 0.6%Pd/Amberlyst A21,[39,40] excellent conversion of **1** and yield of **2** in *A* was obtained after continuous-flow hydrogenation with a Δ*P* of 0.02 MPa. Therefore, 0.6%Pd/Amberlyst A21 was selected for the flow hydrogenation of **1**.

Next, scale-up experiments were conducted for the continuous-flow hydrogenation of **1** using a large column (Table 2). The column size was approximately a 41-fold scale-up (ID: 37 mm; *L*: 300 mm), as shown in Table 1. The flow rates of **1**, AcOH solution, and H_2 gas were also increased. The liquid was passed through a pre-temperature controller prior to entering the reaction column. Because external cooling of the column body was not feasible within the system, the temperature of the incoming liquid was controlled, and the column was operated at ambient temperature. To monitor the internal temperature of the column in detail, two temperature sensors were introduced to record the internal temperature at eight points: four locations along the column centerline (*a*, *c*, *e*, and *g* Table 2) and four near the wall (*b*, *d*, *f*, and *h*, Table 2). When the liquid temperature was controlled at 50 °C, the internal temperatures increased to over 120 °C, and the yield of **2** in *A* was 77% with a Δ*P* of 0.36 MPa. When the

Table 2 Optimisation of continuous-flow hydrogenation of **1** under scale-up conditions

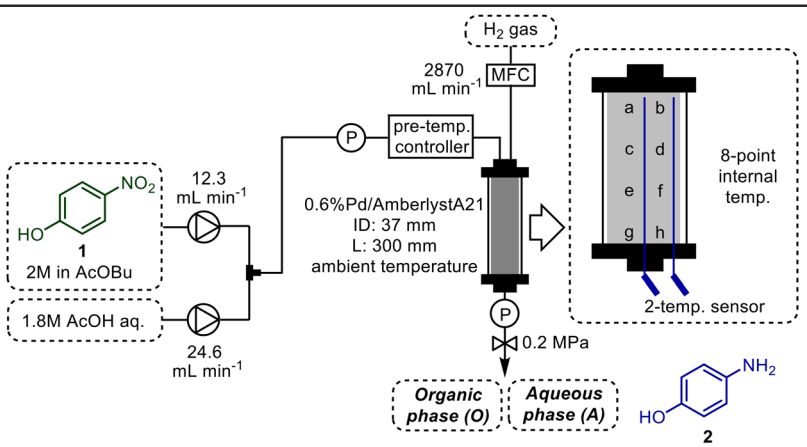

Entry	Pre-temperature controller (°C)	Δ*P* (MPa)	Internal temperature (°C)								Conversion (%)	Yield of **2** in *A* (%)
			a	*b*	*c*	*d*	*e*	*f*	*g*	*h*		
1	50	0.36	41	41	112	83	120	114	128	121	97	77
2	30	0.36	30	28	100	83	121	120	118	116	99	84
3	0	0.36	11	10	67	40	110	83	121	112	98	98

liquid temperature was set to 30 °C, the yield improved to 84%. In these cases, the hydrogenated aromatic rings derived from **2** were observed. In contrast, when the pre-temperature controller was set to 0 °C, maximum internal temperature was 110 °C, and the yield of **2** in *A* was 98% with a ΔP of 0.39 MPa. These results indicate that when the internal temperature in the middle section of the column (internal temperature points *e* and *f*, Table 2) exceeds 120 °C, reduced aromatic species are formed as byproducts, making this a critical parameter for controlling impurity formation. The exothermic heat generated during the hydrogenation of the nitro group is released within the column and does not have a significant impact on Pd catalyst deactivation. Although excess hydrogen is discharged from the column after the reaction, the hydrogenation is carried out in a fume hood, where the gas is promptly diluted and exhausted, ensuring no safety concerns.

Flow acetylation and crystallisation

Next, the acetylation of **2** with Ac_2O and the subsequent crystallisation using a base were investigated (Table 3). The acetylation was carried out in a plug flow reactor (ID: 2.0 mm, *L*: 1115 mm) at 65 °C. A solution of **2** (1.0 M) in 1.8 M aq. AcOH was fed into the plug flow reactor (PFR) at 0.6 mL min^{-1}, and Ac_2O was simultaneously introduced at 0.1 mL min^{-1} (residence time: 3.89 min). The reaction mixture was collected in a flask at −2 °C. Various bases and pH levels for the acetylation and crystallisation processes were investigated. Using potassium hydrogen carbonate ($KHCO_3$) as the base, **3** was obtained in 72.0% yield at pH 6.8. However, $KHCO_3$ gradually decomposed to K_2CO_3, making pH control difficult (entry 1, Table 3). The diacetylated compound **4** formed in 11.5% yield because of the unstable pH conditions. Subsequently, NaOH was employed as the base and acetylation and crystallisation processes were carried out. When the pH was maintained at 8.0, the yields of **3** and **4** were 91.8% and 0.9%, respectively. Next, the optimal pH for the crystallisation of **3** was determined. At pH 6.8, **3** was obtained in 93.1% yield, and the byproduct **4** was obtained in 0.7% yield (entry 3, Table 3). Controlling the pH to 6.0 resulted in a 91.4% yield of **3**, although the formation of **4** was still not negligible (0.6%) (entry 4, Table 3). When the pH was maintained at 5.0, the yields of **3** and **4** were 89.3% and 0.2%, respectively (entry 5, Table 3). Based on these results, pH 5.0 was identified as the optimal condition for acetylation and crystallisation. Finally, integration of the acetylation and crystallisation processes with the flow hydrogenation process was explored.

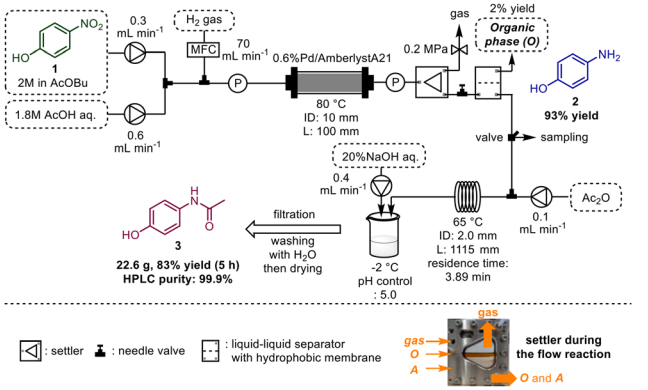

Fig. 2 Continuous synthesis of **3** under small-scale conditions *via* sequential processes.

Integrated process for continuous synthesis of AcAP

Continuous synthesis of **3** *via* the integration of flow hydrogenation, gas–liquid–liquid separation, acetylation, and crystallisation under small-scale conditions was attempted (Fig. 2). Flow hydrogenation was carried out under the conditions listed in Table 1 (entry 11). A settler (MAK Engineering Co. Ltd., MSL-IT-04-00-00) was installed after the hydrogenation step for gas–liquid separation. After the flow reaction, the mixture of gas and liquids (*O* and *A*) was

Table 3 Optimisation of the acetylation of **2** for synthesizing **3**

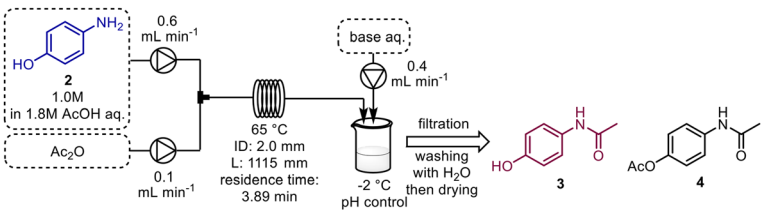

Entry	Base	pH control	Conversion (%)	Yield (%)	
				3	**4**
1	20%$KHCO_3$	6.8[a]	>99	71.6	11.6
2	20%NaOH	8.0	>99	91.8	0.9
3	20%NaOH	6.8	>99	93.1	0.7
4	20%NaOH	6.0	>99	91.4	0.6
5	20%NaOH	5.0	>99	89.3	0.2

[a] pH increased to 8.1 one hour after the base addition was completed at pH 6.8.

successfully separated by controlling the liquid interface using a backpressure regulator and needle valve. The separated liquids, including *O* and *A* solutions, were further separated using a membrane liquid–liquid separator (Zaiput Flow Technologies, SEP-10, with a hydrophobic membrane). Portions of the *O* and *A* solutions were sampled to determine the yield of **2** (*O*: 2% and *A*: 93%). The *A* was directly merged with Ac_2O to proceed to the acetylation process. Acetylation was performed using a PFR, and crystallisation was carried out for 5 h. The obtained solid was filtered and washed with H_2O, affording **3** in 83% yield (22.6 g; HPLC purity: 99.9%).

Finally, a scale-up experiment was conducted for the continuous synthesis of **3** from **1** (Fig. 3). Flow hydrogenation of **1** was carried out under the conditions listed in entry 3, Table 2. After the reaction, the *O* and *A* exhibited poor separation owing to emulsion formation, unlike the clear separation achieved under small-scale conditions. To address this issue, the hydrogenated solution was passed through a coalescer (ID: 55 mm, *L*: 308 mm) packed with glass wool (103.9 g) while releasing the gas. The *O* layer was discharged at a flow rate of 12 mL min^{-1}, whereas the *A* layer was transferred at 26.6 mL min^{-1} and merged with Ac_2O (4.1 mL min^{-1}) for acetylation in a PFR. The acetylation solution containing compound **3** was then cooled in a jacketed reactor maintained at −8 °C to induce crystallisation and form a slurry in vessel A. After 100 minutes, the slurry was transferred to vessel B at 500 mL min^{-1}, and aq. 20% NaOH was added at 16.4 mL min^{-1} until the pH reached 5. The slurry was stirred for an additional 30 min and filtered to obtain **3**. This procedure was repeated three times to yield three batches of **3**, corresponding to a total of 5 h of operation for the acetylation step. The results for the three batches are listed in Table 4. Batches 1 and 2 resulted in approximately 60% yield, whereas batch 3 resulted in 92% yield. These results suggest that crystal classification occurred in vessel A, and that partial transfer to vessel B may have been incomplete. Additionally, 16–18% of **3** was lost during filtration and washing, and a further 3% was lost within vessels A and B. Overall, 775.2 g of crystals were recovered, corresponding to a total yield of 70%.

Process comparison: previous study *vs.* this study

To demonstrate the utility of the developed process, the key parameters—PMI and productivity per unit time—were compared with those reported by Sievers and Bommarius[30] (Table 5). Although their process achieved an excellent PMI of 7.2, the productivity was limited to 7.9 g h^{-1}. Notably, the hydrogenation step employed powdered Pd/Al_2O_3, which presents a significant scale-up challenge owing to its high ΔP.

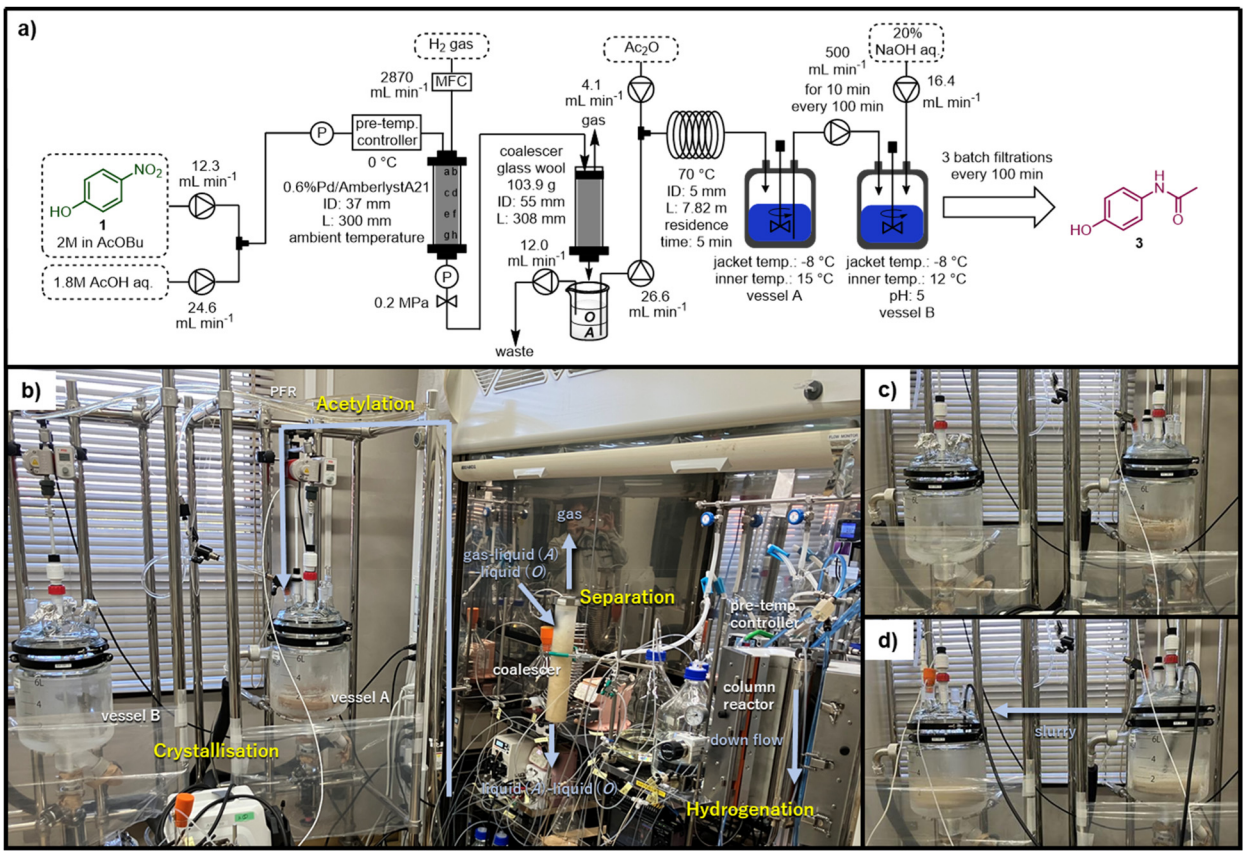

Fig. 3 a) Schematic showing the process flow of the scale-up experiment for continuous synthesis of **3**. b) Reaction setup. c) Slurry in vessel A before transfer. d) Slurry in vessel B after transfer.

Table 4 Results of the scale-up experiment

Batch	Yield [crystal] (g)	Yield [crystal] (%)	HPLC purity [crystal] (%)	Filtrate loss (%)	Loss within vessels A and B (%)
1	221.1	60	99.5	18	
2	216.2	59	99.4	16	
3	337.9	92	99.4	16	
Total =	775.2	70		18	3

Table 5 Comparison of process parameters from a previously reported process with those obtained using the process developed in this study

Process	PMI	Productivity (g h^{-1})
Sievers and Bommarius's process[30]	7.2	7.9
Our process	23.8	155.0

Moreover, nitro-group hydrogenation is exothermic, and temperature control during scale-up has not yet been addressed. A concentration step was also required prior to crystallisation, preventing continuous production of the final crystalline product. In contrast, the flow process developed in this study achieved a higher PMI of 23.8, owing to the use of AcOBu and aq. NaOH for acetylation and neutralisation, respectively. However, we believe these values can be significantly improved by incorporating a solvent recovery process. Additionally, it demonstrated a significantly higher productivity of 155.0 g h^{-1}. Importantly, the developed process enabled continuous production up to the crystallisation step, allowing efficient and rapid synthesis of AcAP directly from 4-NP.

Conclusions

A continuous-flow process for synthesizing AcAP that involves the hydrogenation of 4-NP, inline gas–liquid–liquid separation, acetylation, and crystallization has been successfully developed. The hydrogenation step was efficiently performed using a packed column containing a bead-form 0.6% Pd/Amberlyst A21 catalyst while maintaining a ΔP below 0.4 MPa even under scale-up conditions. Inline separation of the post-hydrogenation gas–liquid mixture enabled the continuous collection of an aqueous solution of 4-AP acetate. Subsequent acetylation with Ac_2O, followed by neutralization with aq. NaOH, allowed for the efficient and continuous production of AcAP. The developed process achieved a PMI of 23.8 and productivity of 155.0 g h^{-1}, demonstrating excellent throughput. Importantly, the developed process integrates crystallization, enabling the direct and continuous production of AcAP from 4-NP in a short time with high efficiency. Ongoing research in our laboratory focuses on collecting detailed crystallization data to further optimise and intensify this continuous manufacturing process.

Conflicts of interest

There are no conflicts to declare.

Data availability

The data supporting this article have been included as part of the supporting information (SI).

Supplementary information: HPLC method, reaction setup, calculation of PMI, energy consumption, and void volume, NMR spectra, HPLC charts. See DOI: https://doi.org/10.1039/d6re00130k.

Acknowledgements

This study was partially supported by the New Energy and Industrial Technology Development Organization (JPNP19004).

Notes and references

1 E. Friderichs, T. Christoph and H. Buschmann, Analgesics and antipyretics, *Ullmann's Encyclopedia of Industrial Chemistry*, ed. B. Elvers, S. Hawkins and G. Schulz, Wiley-VCH Press, Weinheim, Germany, 2012.
2 J. Park, M. A. Kelly, J. X. Kang, S. S. Seemakurti, J. L. Ramirez, M. C. Hatzell, C. Sievers and A. S. Bommarius, Production of active pharmaceutical ingredients (APIs) from lignin-derived phenol and catechol, *Green Chem.*, 2021, **23**, 7488–7498.
3 D. Duan, H. Lei, Y. Wang, R. Ruan, Y. Liu, L. Ding, Y. Zhang and L. Liu, Renewable phenol production from lignin with acid pretreatment and ex-situ catalytic pyrolysis, *J. Cleaner Prod.*, 2019, **231**, 331–340.
4 J. Park, C. Evans, J. Maier, M. Hatzell, S. France, C. Sievers and A. S. Bommarius, Renewables-based routes to paracetamol: A green chemistry analysis, *ACS Sustainable Chem. Eng.*, 2024, **12**, 16271–16282.
5 S. L. Boyall, H. Clarke, T. Dixon, R. W. M. Davidson, K. Leslie, G. Clemens, F. L. Muller, A. D. Clayton, R. A. Bourne and T. W. Chamberlain, Automated optimization of a multistep, multiphase continuous flow process for pharmaceutical synthesis, *ACS Sustainable Chem. Eng.*, 2024, **12**, 15125–15133.
6 P. Roche, R. C. Jones, B. Glennon and P. Donnellan, Development of a continuous evaporation system for an API solution stream prior to crystallization, *AIChE J.*, 2021, **67**, e17377.
7 Y. C. Liu, A. Domokos, S. Coleman, P. Firth and Z. K. Nagy, Development of continuous filtration in a novel continuous filtration carousel integrated with continuous crystallization, *Org. Process Res. Dev.*, 2019, **23**, 2655–2665.
8 S. D. Karlen, V. I. Timokhin, C. Sener, J. K. Mobley, T. Runge and J. Ralph, Production of biomass-derived *p*-Hydroxybenzamide: synthesis of *p*-aminophenol and paracetamol, *ChemSusChem*, 2024, **17**, e202400234.

9 M. Jiang and X.-W. Ni, Reactive crystallization of paracetamol in a continuous oscillatory baffled reactor, *Org. Process Res. Dev.*, 2019, **23**, 882–890.
10 F. A. Khan, J. Dash, C. Sudheer and R. K. Gupta, Chemoselective reduction of aromatic nitro and azo compounds in ionic liquids using zinc and ammonium salts, *Tetrahedron Lett.*, 2003, **44**, 7783–7787.
11 K. M. Doxsee, M. Feigel, K. D. Stewart, J. W. Canary, C. B. Knobler and D. J. Cram, Host–Guest complexation. 42. Preorganization strongly enhances the Tendancy of Hemispherands to form Hemispheraplexes, *J. Am. Chem. Soc.*, 1987, **109**, 3098–3107.
12 K. Kubota, A. Nagao and H. Ito, Solvent-free zinc-mediated Béchamp reduction using mechanochemistry, *RSC Mechanochem.*, 2025, **2**, 389–393.
13 C. A. Merlic, S. Motamed and B. Quinn, Structure determination and synthesis of fluoro nissl green: an RNA-binding fluorochrome, *J. Org. Chem.*, 1995, **60**, 3365–3369.
14 R. Porcar, A. Mollar-Cuni, D. Ventura-Espinosa, S. V. Luis, E. García-Verdugo and J. A. Mata, A simple, Safe and Robust System for Hydrogenation "without High-Pressure Gases" under Batch and Flow Conditions Using a Liquid Organic Hydrogen Carrier, *Green Chem.*, 2022, **24**, 2036–2043.
15 I. R. Baxendale, L. Brocken and C. J. Mallia, Flow chemistry approaches directed at improving chemical synthesis, *Green Process. Synth.*, 2013, **2**, 211–230.
16 D. Sui, F. Mao, H. Fan, Z. Qi and J. Huang, General reductive amination of aldehydes and ketones with amines and nitroaromatics under H_2 by recyclable iridium catalysts, *Chin. J. Chem.*, 2017, **35**, 1371–1377.
17 J. Gardiner, X. Nguyen, C. Genet, M. D. Horne, C. H. Hornung and J. Tsanaktsidis, Catalytic static mixers for the continuous flow hydrogenation of a key intermediate of linezolid (Zyvox), *Org. Process Res. Dev.*, 2018, **22**, 1448–1452.
18 B. Venezia, L. Panariello, D. Biri, J. Shin, S. Damilos, A. N. P. Radhakrishnan, C. Blackman and A. Gavriilidis, Catalytic Teflon AF-2400 membrane reactor with adsorbed ex situ synthesized Pd-based nanoparticles for nitrobenzene hydrogenation, *Catal. Today*, 2021, **362**, 104–112.
19 M. Pietrowski, M. Zieliński, E. Alwin, I. Gulaczyk, R. E. Przekop and M. Wojciechowska, Cobalt-doped magnesium fluoride as a support for platinum catalysts: the correlation of surface acidity with hydrogenation activity, *J. Catal.*, 2019, **378**, 298–311.
20 X. Duan, X. Wang, X. Chen and J. Zhang, Continuous and selective hydrogenation of heterocyclic nitroaromatics in a micropacked bed reactor, *Org. Process Res. Dev.*, 2021, **25**, 2100–2109.
21 X. Duan, J. Yin, A. Feng, M. Huang, W. Fu, W. Xu, Z. Huang and J. Zhang, Continuous hydrogenation of halogenated nitroaromatic compounds in a micropacked bed reactor, *J. Flow Chem.*, 2022, **12**, 121–129.
22 K. Chai, R. Shen, T. Qi, J. Chen, W. Su and A. Su, Continuous-flow hydrogenation of nitroaromatics in microreactor with mesoporous Pd@SBA-15, *Processes*, 2023, **11**, 1074.
23 A. Reina, I. Favier, E. Teuma, M. Gómez, A. Conte and L. Pichon, Hydrogenation reactions catalyzed by colloidal palladium nanoparticles under flow regime, *AIChE J.*, 2019, **65**, e16752.
24 R. J. Gulotty, S. Rish, A. Boyd, L. Mitchell, S. Plageman, C. McGill, J. Keller, J. Starnes, J. Stadalsky and G. Garrison, Run parameters for a continuous hydrogenation process using ACMC-Pd to replace commercial batch reactor processes, *Org. Process Res. Dev.*, 2018, **22**, 1622–1627.
25 J. N. Appaturi, R. Ratti, B. L. Phoon, S. M. Batagarawa, I. U. Din, M. Selvaraj and R. J. Ramalingam, A review of the recent progress on heterogeneous catalysts for Knoevenagel condensation, *Dalton Trans.*, 2021, **50**, 4445–4469.
26 J. C. Pastre, D. L. Browne and S. V. Ley, Flow chemistry syntheses of natural products, *Chem. Soc. Rev.*, 2013, **42**, 8849–8869.
27 K. Masuda, T. Ichitsuka, N. Koumura, K. Sato and S. Kobayashi, Flow fine synthesis with heterogeneous catalysts, *Tetrahedron*, 2018, **74**, 1705–1730.
28 A. Tanimu, S. Jaenicke and K. Alhooshani, Heterogeneous catalysis in continuous flow microreactors: a review of methods and applications, *Chem. Eng. J.*, 2017, **327**, 792–821.
29 C. G. Thomson, A.-L. Lee and F. Vilela, Heterogeneous photocatalysis in flow chemical reactors, *Beilstein J. Org. Chem.*, 2020, **16**, 1495–1549.
30 J. Park, M. Hatzell, C. Sievers and A. S. Bommarius, Simultaneous hydrogenation and acetylation of 4-nitrophenol in a two-stage packed-bed reactor as a process intensification strategy for highly selective paracetamol synthesis, *ACS Sustainable Chem. Eng.*, 2025, **13**, 5906–5915.
31 J. Krueger, A. P. Dieskau, J. Hassfeld, J. Gries, O. Block, H. Weinmann, D. Kaufmann, S. Hildbrand, V. Kraft, R. Moeckel, J. R. Dehli, U. Scholz and C. F. Nising, Chemical process development in the pharmaceutical industry in Europe—insights and perspectives from industry scientists, *Angew. Chem., Int. Ed.*, 2025, **64**, e202420719.
32 G. Cravotto, Reshaping chemical manufacturing towards green process intensification: recent findings and perspectives, *Processes*, 2025, **13**, 459.
33 S. E. Raby-Buck, J. Devlin, P. Gupta, C. Battilocchio, M. Baumann, A. Polyzos, A. G. Slater and D. L. Browne, Continuous flow chemistry for molecular synthesis, *Nat. Rev. Methods Primers*, 2025, **5**, 44.
34 K. Masuda, T. Yamamoto, K. Kobayashi, H. Sano, I. Saito, A. Nagaki and A. Yada, Crystallization-based approach to continuous manufacturing: a case study of acetaminophen production, *Org. Process Res. Dev.*, 2026, **30**, 312–320.
35 K. P. Cole, J. M. Groh, M. D. Johnson, C. L. Burcham, B. M. Campbell, W. D. Diseroad, M. R. Heller, J. R. Howell, N. J. Kallman, T. M. Koenig, S. A. May, R. D. Miller, D. Mitchell, D. P. Myers, S. S. Myers, J. L. Phillips, C. S. Polster, T. D. White, J. Cashman, D. Hurley, R. Moylan, P. Sheehan, R. D. Spencer, K. Desmond, P. Desmond and O. Gowran, Kilogram-Scale Prexasertib Monolactate Monohydrate Synthesis under Continuous-Flow CGMP Conditions, *Science*, 2017, **356**, 1144–1150.

36 R. Parvaresh and Z. K. Nagy, Process Intensification via End-to-End Continuous Manufacturing of Atorvastatin Calcium Using an Integrated, Modular Reaction-Crystallization-Spherical Agglomeration-Filtration-Drying Process, *Org. Process Res. Dev.*, 2024, **28**, 2906–2918.

37 M. Jiang, M. Liu, W. Li, Y. Xia and F.-E. Chen, An Eight-Step Continuous-Flow Total Synthesis of Vitamin B1, *Engineering*, 2024, **32**, 226–232.

38 N. L. R. Susarla, D. J. R. Velaga, M. Y. Sardar, A. Ghosh, R. K. Gorle, S. Jawlekar, R. R. Budhdev and S. Ramakrishnan, Continuous Crystallization of Atorvastatin Calcium at a Multitonnage Scale Using Dynamically Mixed Flow Reactors for Target Polymorph Control, *Org. Process Res. Dev.*, 2025, **29**, 1662–1676.

39 N. P. Allen, F. O. Bamiro, R. P. Burns, J. Dywer and C. A. McAuliffe, Catalytic reactions involving palladium(II) salts supported on Amberlyst, *Inorg. Chim. Acta*, 1978, **28**, 231–235.

40 S. Nagireddi, A. K. Golder and R. Uppaluri, Role of protonation and functional groups in Pd(II) recovery and reuse characteristics of commercial anion exchange resin-synthetic electroless plating solution systems, *J. Water Process Eng.*, 2018, **22**, 227–238.

